

Performance of Sparse Code Multiple Access Communication System Based on Logarithmic Message Passing Algorithm and Low-Density Parity Check Code

Mustafa Safwan Moafaq*, Maher K. Mahmood Al-Azawi

Electrical Engineering Department, College of Engineering, Mustansiriyah University, Baghdad, Iraq

Correspondance

*Mustafa Safwan Moafaq

Electrical Engineering Department, College of Engineering,
Mustansiriyah University, Baghdad, Iraq

Email: Mustafa.S.Moafaq@uomustansiriyah.edu.iq

Abstract

The performance of Sparse Code Multiple Access (SCMA) communication system with Logarithmic Message Passing Algorithm (log-MPA) decoder is introduced. To boost the performance, a Low-Density Parity-Check Code LDPC is used together with Belief Propagation (BP) decoder. LDPC is chosen due to its sparsity property that complements the sparsity nature of SCMA for maximum efficiency and minimum complexity. Three distinct SCMA configurations are used. These are: A ($4 \times 4 \times 6$), B ($4 \times 16 \times 6$), and C ($5 \times 4 \times 10$) where the ($K \times M \times V$) are numbers of resources, codewords and users respectively. The performance of these configuration is shown in various channel conditions, various LDPC code rates and various numbers of SCMA iterations (N_{SCMA}), to find the local minimum value of log-MPA. Simulation results showed that the LDPC greatly boosted the performance in mentioned configurations: In A configuration, a gain of 13 dB was observed. Configuration B experienced a substantial improvement of 23.5 dB, while C achieved a gain of 20.5 dB. Notably, configuration B stood out with the highest gain, attributed to LDPC's exceptional performance with high data rates, as the data transmitted in B was double that of A.

Keywords

Non-Orthogonal Multiple Access, NOMA, Sparse Code Multiple Access, Logarithmic Message Passing Algorithm, Low-Density Parity Check Code.

I. INTRODUCTION

In recent years, the number of internet users has been steadily rising. This increase has fueled a growing demand for higher data rates, improved spectral efficiency, and overall enhanced user experiences. Unlike the techniques employed in previous generations, Non-Orthogonal Multiple Access (NOMA) introduces a departure from conventional methods. In 1G through 3G systems, communication relied on Orthogonal Multiple Access (OMA) resources, where the orthogonality was in frequency, time or code [1]. In the context of 4G systems, Orthogonal Frequency Division Multiple Access (OFDMA) plays a pivotal role in managing multiple users by allocating them to specific subsets of sub-carriers,

thus mitigating interference issues. Nevertheless, the spectral efficiency of OFDMA is constrained by the necessity to maintain sufficient carrier spacing to preserve the orthogonality among sub-carriers. However, to fulfill the demands of 5G networks, Non-Orthogonal Multiple Access (NOMA) has emerged as a promising candidate. This utilization of non-orthogonal resources marks a major transformation in approach. L. Dai, B. Wang et al. [2] showed the difference between OMA and NOMA in terms of channel capacity. This paradigm shift opens up new avenues for optimizing spectral efficiency [3] and accommodating a diverse range of user requirements, from low-latency machine-type communications to high-throughput multimedia streaming. With its potential



This is an open-access article under the terms of the Creative Commons Attribution License, which permits use, distribution, and reproduction in any medium, provided the original work is properly cited.
©2025 The Authors.

Published by Iraqi Journal for Electrical and Electronic Engineering | College of Engineering, University of Basrah.

to revolutionize the way future wireless networks are designed and operated with NOMA system that stands at the forefront of next-generation communication technologies, promising to unlock unprecedented levels of connectivity and performance for the Internet of Things (IoT) [4], 5G and beyond. The subject of NOMA has undergone substantial scrutiny in the past decade, with comprehensive studies spanning all three categories: power domain, code domain, and hybrid domain. The key difference between power and code domain multiplexing is that the latter can achieve greater spreading and shaping gains, resulting in an increase in channel capacity at the expense of signal bandwidth [2]. Code domain is a sub-category of NOMA and it has many techniques under its umbrella, including: Low Density Signature (LDS)-Orthogonal Frequency Division Multiplexing (OFDM) [5], LDS-Code Division Multiple Access CDMA [6] and SCMA [7]. The main focus of this paper is Spare Code Multiple Access (SCMA) which is the most prominent and advanced technique in the code domain category. SCMA was first introduced by Huawei in 2013 [7] as a more sophisticated multiplexing method as opposed to (LDS) [8]. Due to the sparsity of the codebooks, SCMA still uses the low complexity receiver that LDS has, such as, Message Passing Algorithm (MPA) [9] but with greater improvements in the performance. As proved by Y. Wu, S. Zhang [9], MPA is the best detection technique in SCMA up to an overloading factor ($f_{\text{overload}} = V / K$) of 3, where V , K represents number of users and resources respectively. In this paper, a simpler and more energy efficient version of MPA is used, log-MPA [10], which replaces the multiplication and exponent by addition and optimization respectively. To get even better performance, an error-correcting code is considered. This can be turbo codes, density parity check (LDPC) codes or polar codes [11], in this paper, LDPC code is used for this purpose. LDPC codes are used due to its high error-correcting ability, low complexity, as proven in [12], as it uses the sparse property and hence its ability to be implemented by FPGA systems easier than other Forward Error-Correction Codes (FEC) codes. Therefore, it seems that the combined utilization of LDPC and SCMA will be implemented in practical applications within network systems in the future.

Table I is a summary of what was shown in [12] and [13]. From it, we can see that LDPC codes offer a robust solution for SCMA due to their structure that works well with sparse data, strong performance, and reasonable complexity. Although polar and turbo codes have their merits, LDPC strikes an optimal trade-off for SCMA use.

TABLE I.
COMPLEXITY AND PERFORMANCE COMPARISON
BETWEEN DIFFERENT ERROR-CORRECTION CODES

Code Type	Encoding Complexity	Decoding Complexity	Performance	Reference
Turbo Code	Moderate	High (Viterbi or BCJR)	Close to capacity limit	[14]
Polar Code	Moderate	Low (Successive Cancellation)	Near capacity with careful design	[15]
LDPC Code	Low	Moderate	Good performance, sparsity-friendly	[16]

With that being said, SCMA has some drawbacks and difficulties in real world implementation. These include: firstly, the complexity aspect, which leads to higher costs and number of operations and these numbers get even higher by adding LDPC code as it also requires an iterative decoding algorithm similar to SCMA. Secondly, since SCMA is still a new subject, standardization and interoperability with current communication systems is challenging. Lastly, accurate estimation [17] of the channel coefficients of each user can be difficult due to the overlapping of multiple users on a single resource. These challenges can be addressed through further research and experimentation in the field. Specifically, the optimization of codebook and receiver designs. This paper examines various SCMA configurations, each accompanied by different LDPC code rates, providing an overview of how the system behaves when the number of users, resources and the length of stream bits are adjusted. Additionally, it presents different iteration numbers for the SCMA decoding algorithm. This paper is organized as follows: an overview of SCMA is given in section II. . An overview of LDPC is explained in section III. . The system model and log-MPA's Log Likelihood Ratio (LLR) equations' derivation are given in section IV. . Section V. presents the simulation results. Finally, section VI. gives some conclusion points.

II. SPARSE CODE MULTIPLE ACCESS (SCMA)

The main idea of SCMA is utilizing non-orthogonal code channel separation. The best way to describe SCMA is by using a factor graph (or Tanner graph) that consists of User

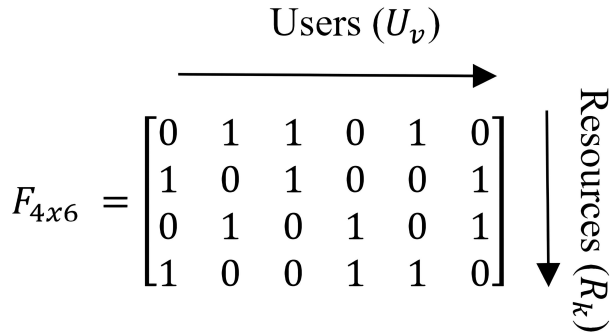


Fig. 1. Indicator matrix for 4 resources and 6 users SCMA. Where $v = 1, \dots, 6$ and $k = 1, \dots, 4$

Nodes (UNs) and Resource Nodes (RNs). Each user node is connected to d_r resource node. And each resource node is connected to d_c users. Both d_r and d_c control the sparsity (number of non-zero elements in each column and row, respectively) in the factor graph (indicator) matrix, $f_{K \times V}$. Where, no rows or columns can be the same to avoid inter-user interference. Fig. 1 shows an example of indicator matrix and its Tanner graph, where $K=4$, $V=6$, $d_r=2$ and $d_c=3$.

Indicator matrix, F , is used for resource allocation i.e. in Fig. 1 the first column has two non-zero elements in the 2nd and 4th rows, meaning, user 1's (U_1) data is assigned to be transmitted on the 2nd and 4th resource. Similarly for remaining users This can be easily seen in Fig. 2. The core of SCMA centers around two major concepts:

1. The utilization of Codebooks (CBs), which are, 3-D ($K \times M \times V$) sparse, complex ($CB \subset \mathbb{C}$) matrices. Here, each dimension represents: number of resources (K), codewords (M) and users (V), respectively. Each user (v) must have a unique ($K \times M$) CB to avoid interference. The design of such CBs needs to be optimized as they have a huge impact on the

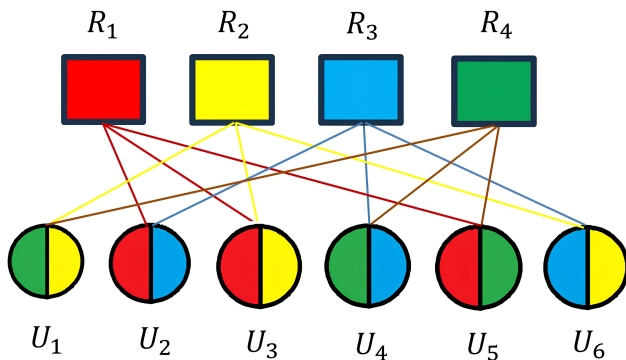


Fig. 2. Tanner graph of Fig. 1

shaping gain.

2. The detection technique used in SCMA is crucial for accurately extracting transmitted signals from the received data amidst multi-user interference. This detection process entails decoding the sparse structure of the received signal to isolate the intended symbols aiming to enhance both the accuracy and efficiency of signal recovery. The selection of an appropriate detection technique is the key, as it profoundly influences the overall performance and reliability of SCMA systems. All techniques used in SCMA are MPA-based algorithms. The development of SCMA is dependent on new researches in both CB design and decoding algorithms [18].

In this paper, three SCMA configurations have been examined: ($4 \times 4 \times 6$), ($4 \times 16 \times 6$), ($5 \times 4 \times 10$). The first two configurations are subjected to a 150% overload scenario, while the last configuration experiences a 200% overload condition. An overloading of 200% is complicated due to several reasons. In SCMA, which relies on sparse Codebooks CBs and unique signature sequences for users, accommodating overloading while maintaining low interference and complexity in decoding is particularly challenging. The presence of additional users can cause inter-user interference, necessitating more sophisticated receiver algorithms capable of successfully mitigating such effects. Moreover, decoding complexity escalates as the receiver needs to perform joint detection of signals from multiple users sharing the same resources. However, in the second configuration, the same log-MPA is employed for the purpose of a fair comparison.

III. LOW DENSITY PARITY CHECK CODE (LDPC)

LDPC codes are Forward Error-Correction (FEC) codes and was conceptualized by Robert Gallager in 1960. They were first introduced in a book in 1963 [16]. LDPC codes were overlooked at the time they appeared due to: their high computational complexity and the dominance of convolutional codes in the realm of FEC codes. However, in the early 2000s, LDPC codes began to gain significant attention and practical usage in public systems. A notable example occurred in digital video broadcasting (DVB-S2), where LDPC codes were embraced as the FEC scheme for satellite television transmission [19]. Since then, LDPC codes have been widely utilized in different communication systems and standards, including Wi-Fi (IEEE 802.11n and later) [20], 4G LTE, and 5G NR (New Radio). LDPC codes main operation scheme is adding redundancy to the transmitted data, which achieves error detection and correction. The encoding process involves dividing the input data into blocks and calculating parity bits based on a sparse parity-check matrix (H). At the receiver end, LDPC decoding algorithms, such as Belief Propagation

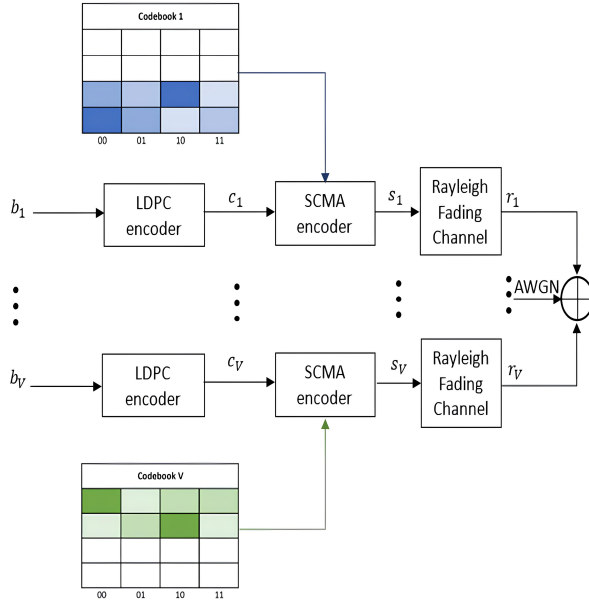


Fig. 3. SCMA-LDPC transmitter and channel

(BP) [21] and Sum-Product Algorithm (SPA), iteratively refine estimates of the original message, leveraging the structure of the parity-check matrix (H) to efficiently correct errors caused by channel noise. LDPC codes are renowned for their near-optimal error-correction performance, particularly at high data rates and low signal-to-noise ratios [22].

IV. SYSTEM MODEL

A. Transmitter and Channel

The transmitter plus a Rayleigh channel communication system with SCMA as the multiplexing scheme and LDPC as the error-correcting code are shown in Fig. 3.

The system takes the information bits stream (b_v), where, $v = 1, \dots, V$, with length of $\log_2(M)$ bits as input to the LDPC encoders. Then the LDPC encoder adds parity check bits depending on its code rate. Afterwards, the coded word (c_v) is sent to the SCMA encoder. Depending on the coded word, s_v is determined by a selection process and it is done by grabbing the codewords (Columns) of the CB. For instance, consider a scenario where the codebook has dimensions $K=4$ and $M=4$, the length of data would be $\log_2(4)=2$ bits. Subsequently, if the coded word is "00", the first column of the codebook is selected. Similarly, if data is "01", the second column of the codebook is chosen. And so on. Next, the complex code-word (s_v) obtained from previous step is then multiplied by a Rayleigh channel coefficient to get r_v . In wireless communications, diversity techniques (time, frequency or antenna) can be used to reduce the effect of Rayleigh fading [23]. Finally, by

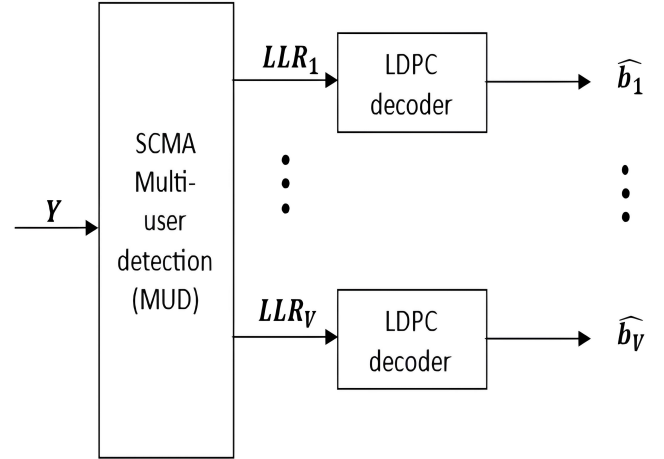


Fig. 4. SCMA-LDPC receiver

summing r_v for all values of v and adding the AWGN effect, the combined signal, Y , is ready for reception.

$$Y = \sum_v \text{diag}(h_v) \cdot \text{CB}_v(x_v) + n \quad (1)$$

where x_v defines the information bits sent by the v^{th} user; CB_v is the codebook of user v ; the term $\text{CB}_v(x_v)$ represents a vector (column) of the codebook of user v determined by users' data x_v ; h_v is the Rayleigh channel vector faced by user v ; n is the AWGN.

B. Receiver

The SCMA-LDPC receiver is shown in Fig. 4.

The process begins with the received signal, denoted as Y , entering the Multi-User Detection (MUD) system. Within the MUD, an iterative Message Passing Algorithm (MPA) is employed to extract the Log Likelihood Ratio (LLR) through Log-MPA. Each LLR value, denoted as $(\text{LLR})_v$, corresponds to the number of bits in the data, represented by $\log_2(M)$. Subsequently, these LLR values are fed into the LDPC decoder to accurately decode the received bits. The LDPC decoder utilizes a soft decoding technique known as Belief Propagation (BP). This iterative technique has many forms. In this paper, a Layered BP [21] is used. The MPA for an SCMA decoding system with 4 resources and 6 users is demonstrated below:

1. Initialization: At the receiver side, the received vector Y and the Rayleigh channel coefficients have to be known. The likelihood ratio (ψ) is calculated at each Resource Node (RN). Let's assume RN_l where $l=1, \dots, K$, which has three users' data superimposed $\xi_{l1}=\{v_1, v_4, v_5\}$. Hence, the likelihood function at RN_l will be $\psi(y_l | x_1, x_4, x_5, N_0)$ where,

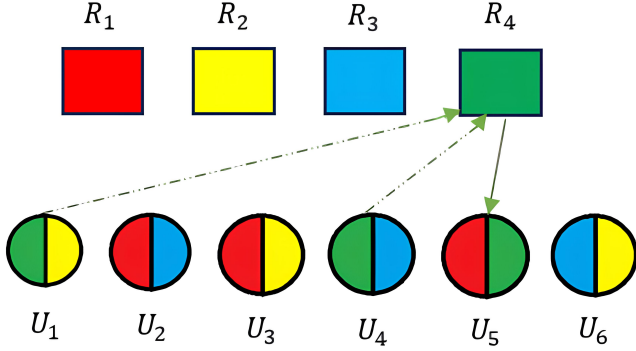


Fig. 5. Message Passing from RN to UN

x_1, x_4, x_5 are the codewords sent by users that belongs to set ξ_l which are connected to R_4 in Fig. 2. Suppose that the set of codeword elements allocated to user v on resource element l is represented as $CB(l, v)$. The likelihood function of RN_l is given by [18]:

$$\psi(y_l | x_1, x_4, x_5, N_0) = \exp \left(\frac{-1}{N_0} \|y_l - (h_{l1}x_{l,1} + h_{l4}x_{l,4} + h_{l5}x_{l,5})\|^2 \right) \quad (2)$$

$$\text{for } x_{l,1} \in CB_{l,1}, x_{l,4} \in CB_{l,4}, x_{l,5} \in CB_{l,5}$$

In this context, $x_{(l,v)}$, $h_{(l,v)}$ represents the codeword element transmitted and Rayleigh channel coefficient faced by the v^{th} user on the l^{th} resource element. N_0 is the variance of noise in AWGN. A total of KM^{dc} values are stored for the function $\psi(y_l | x_1, x_4, x_5, N_0)$. For an uncoded SCMA system, let's assume equal prior probability for each codeword, meaning $P(x_1) = P(x_4) = P(x_5) = 1/M$. Consequently, the initial message passed (η^{init}) from User Node (UN) v_1, v_4, v_5 to the l^{th} RN is:

$$\begin{aligned} \eta_{v_1 \rightarrow l}^{init}(x_1) &= \eta_{v_4 \rightarrow l}^{init}(x_4) \\ &= \eta_{v_5 \rightarrow l}^{init}(x_5) = \frac{1}{M} \end{aligned} \quad (3)$$

2. Update RN: Let's consider $\xi_l = \{v_1, v_4, v_5\}$. where v_1, v_4 , and v_5 represent the three users connected to RN_l , respectively. When passing the message from RN to one user, the information received on the RN from the other two users can be viewed as extrinsic information, as illustrated in Fig. 5.

Message passed from RN_l to U_1 is given as:

$$\begin{aligned} \eta_{l \rightarrow v_1}(x_1) &= \sum_{x_4 \in CB_4} \sum_{x_5 \in CB_5} \\ &(\psi(y_l | x_1, x_4, x_5, N_0) \times \eta_{v_4 \rightarrow l}(x_4) \eta_{v_5 \rightarrow l}(x_5)) \end{aligned} \quad (4)$$

$$\text{for } x_1 \in CB_1$$

In equation (4), the messages from the two RNs, denoted as $\eta_{v_4 \rightarrow l}(x_4)$ and $\eta_{v_5 \rightarrow l}(x_5)$, are multiplied by the local likelihood function of the l^{th} RN and then marginalized with respect to v_1 . Similarly, the messages passed from RN_1 to UNs v_4 and v_5 , respectively, are:

$$\begin{aligned} \eta_{l \rightarrow v_4}(x_4) &= \sum_{x_1 \in CB_1} \sum_{x_5 \in CB_5} \\ &(\psi(y_l | x_1, x_4, x_5, N_0) \times \eta_{v_1 \rightarrow l}(x_1) \eta_{v_5 \rightarrow l}(x_5)) \end{aligned} \quad (5)$$

$$\text{for } x_4 \in CB_4$$

$$\begin{aligned} \eta_{l \rightarrow v_5}(x_5) &= \sum_{x_1 \in CB_1} \sum_{x_4 \in CB_4} \\ &(\psi(y_l | x_1, x_4, x_5, N_0) \times \eta_{v_1 \rightarrow l}(x_1) \eta_{v_4 \rightarrow l}(x_4)) \end{aligned} \quad (6)$$

$$\text{for } x_5 \in CB_5$$

Messages passing from RN_l to UN_v represents the estimate of the received signal for all possibilities of UN_v .

3. Update UN: Let's consider $\zeta_v = \{l_1, l_2\}$ which represents U_3 in Fig. 2 where l_1, l_2 are the resources connected to UN_v . Message passing from UN_v to RN_{l_1} and RN_{l_2} are:

$$\eta_{v \rightarrow l_1}(x_v) = \text{normalize} (P_a(x_v) \eta_{l_2 \rightarrow v}(x_v)) \quad (7)$$

$$\text{for } x_v \in CB_v$$

$$\eta_{v \rightarrow l_2}(x_v) = \text{normalize} (P_a(x_v) \eta_{l_1 \rightarrow v}(x_v)) \quad (8)$$

$$\text{for } x_v \in CB_v$$

Where P_a is the prior probability of user v and $\eta_{l_2 \rightarrow v}$ denotes the updates UN_v obtained from RN_{l_2} . Here, it is required to normalize to make sure that every belief stays within the range of [0,1]. So, (7) can be rewritten as:

$$\eta_{v \rightarrow l_1}(x_v) = \frac{P_a(x_v) \eta_{l_2 \rightarrow v}(x_v)}{\sum_{x_v} \eta_{l_2 \rightarrow v}(x_v)} \quad (9)$$

Message passing from user nodes to resource nodes is shown in Fig. 6 which represents the communication between UN_v and RN_{l_2} . Due to the cyclic nature of the factor graph, messages are exchanged between RNs and UNs repeatedly

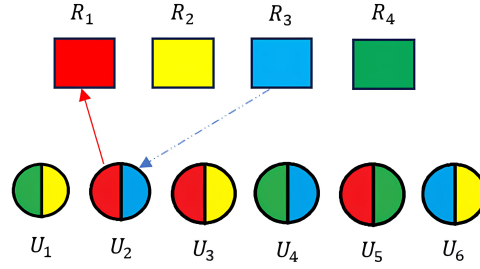


Fig. 6. Message Passing from UN to RN

over several iterations. This process continues until there's zero or a little alteration in the beliefs computed at each UN.

4. Selection of Beliefs and LLR Calculations: After carrying out Steps 2 and 3 for N_{SCMA} iterations, the ultimate belief is determined at each UN. This belief is derived from the prior probability and the messages received from adjacent RNs associated with each UN.

$$I_v(x_v) = P_a(x_v) \eta_{l_1 \rightarrow v}(x_v) \eta_{l_2 \rightarrow v}(x_v) \quad (10)$$

for $x_v \in CB_v$

At each UN, the probability for every possible codeword is calculated. Then, the codeword with the highest probability is selected as the estimated one for that user. This method gives us one way to estimate what was transmitted for each user. Another approach involves computing the LLR for each bit from $I_v(x_v)$. So, the LLR for the i^{th} bit at UN v can be expressed as follows:

$$\begin{aligned} LLR(b_v^i) &= \log \frac{P(b_v^i = +1)}{P(b_v^i = -1)} \\ &= \log \left(\frac{\sum_{x_v | b_v^i = +1} I_v(x_v)}{\sum_{x_v | b_v^i = -1} I_v(x_v)} \right) \quad (11) \\ &\text{for } i = 1, \dots, \log_2(M) \end{aligned}$$

For the case of $M = 4$, we have two bits per symbol. Let $CB_v = \{x_v^1, x_v^2, x_v^3, x_v^4\}$ represent the four codewords corresponding to the four symbols $\{s^1, s^2, s^3, s^4\}$ that user v can send. By applying (10), the final belief for each of the four codewords is computed. Then, LLR for the first bit can be expressed as:

$$\begin{aligned} LLR(b_v^1) &= \log \frac{P(b_v^1 = +1)}{P(b_v^1 = -1)} \\ &= \log \left(\frac{I_v(x_v^1) + I_v(x_v^2)}{I_v(x_v^3) + I_v(x_v^4)} \right) \quad (12) \end{aligned}$$

The ratio of the computed belief corresponding to codewords x_v^1, x_v^2 and x_v^3, x_v^4 provides the LLR for the first bit. Likewise,

for the second bit the LLR is given by:

$$LLR(b_v^2) = \log \left(\frac{I_v(x_v^1) + I_v(x_v^3)}{I_v(x_v^2) + I_v(x_v^4)} \right) \quad (13)$$

The same procedure can be done for the $M = 16$ configuration as it has $\log_2(M) = 4$ LLR values. The LLR values are derived similarly and the results are given as follows:

Algorithm 1 SCMA-LDPC Algorithm

Inputs:

CB_j : Codebook of the j -th user, $\forall j = 1, \dots, J$

N_{SCMA} : Number of the decoding algorithm for SCMA

N_{LDPC} : Number of the decoding algorithm for LDPC

P : Prototype matrix for LDPC

Z : Subblock size of LDPC

Outputs:

Estimated bits for the j -th user, $\forall j = 1, \dots, J$

Initialization:

1. Calculate Signal-to-Noise ratio: $SNR = \frac{E_b}{N_0} + 10 \log_{10} \left(\log_2(M) \frac{V}{K} \right)$, where K, V, M are: number of resources, users, and codewords respectively.
2. Calculate noise power: $N_0 = \frac{P_{signal}}{P_{noise}}$
3. Generate information bits.

Step 1: LDPC Encoding

Create the parity check matrix H using P and Z .

Encode the generated data using H to get the coded word of the j -th user (C_j), $\forall j = 1, \dots, J$.

Divide the coded word into blocks of size BS .

Step 2: SCMA Encoding & Decoding

for $i = 1$ to BS do

- 2.1 Generate Rayleigh channel coefficients (h).
- 2.2 SCMA Mapping using eq. (1).
- 2.3 Adding AWGN effect
- 2.4 Calculating LLR values using Algorithm 2

end for

For the 1st bit:

$$LLR(b_v^1) = \log \left(\frac{I_v(x_v^1) + I_v(x_v^2) + I_v(x_v^3) + I_v(x_v^4) + I_v(x_v^5) + I_v(x_v^6) + I_v(x_v^7) + I_v(x_v^8)}{I_v(x_v^9) + I_v(x_v^{10}) + I_v(x_v^{11}) + I_v(x_v^{12}) + I_v(x_v^{13}) + I_v(x_v^{14}) + I_v(x_v^{15}) + I_v(x_v^{16})} \right) \quad (14)$$

For the 2nd bit:

$$LLR(b_v^2) = \log \left(\frac{I_v(x_v^1) + I_v(x_v^2) + I_v(x_v^3) + I_v(x_v^4) + I_v(x_v^9) + I_v(x_v^{10}) + I_v(x_v^{11}) + I_v(x_v^{12})}{I_v(x_v^5) + I_v(x_v^6) + I_v(x_v^7) + I_v(x_v^8) + I_v(x_v^{13}) + I_v(x_v^{14}) + I_v(x_v^{15}) + I_v(x_v^{16})} \right) \quad (15)$$

For the 3rd bit:

$$LLR(b_v^3) = \log \left(\frac{I_v(x_v^1) + I_v(x_v^2) + I_v(x_v^5) + I_v(x_v^6) + I_v(x_v^9) + I_v(x_v^{10}) + I_v(x_v^{13}) + I_v(x_v^{14})}{I_v(x_v^3) + I_v(x_v^4) + I_v(x_v^7) + I_v(x_v^8) + I_v(x_v^{11}) + I_v(x_v^{12}) + I_v(x_v^{15}) + I_v(x_v^{16})} \right) \quad (16)$$

For the 4th bit:

$$LLR(b_v^4) = \log \left(\frac{I_v(x_v^1) + I_v(x_v^3) + I_v(x_v^5) + I_v(x_v^7) + I_v(x_v^9) + I_v(x_v^{11}) + I_v(x_v^{13}) + I_v(x_v^{15})}{I_v(x_v^2) + I_v(x_v^4) + I_v(x_v^6) + I_v(x_v^8) + I_v(x_v^{10}) + I_v(x_v^{12}) + I_v(x_v^{14}) + I_v(x_v^{16})} \right) \quad (17)$$

Using results from (14), (15), (16) and (17), these LLR values will be the inputs to the LDPC decoders. Afterwards, a soft or a hard decision is made.

The algorithms for the SCMA-LDPC with Max-log-MPA as the decoding technique can be seen in Algorithm 1 and Algorithm 2.

V. SIMULATION RESULTS

Table II shows the simulation parameters and notations used.

TABLE II.
SIMULATION PARAMETER NOTATION

Parameter	Notation
Number of users	V
Number of resources	K
Number of codewords	M
Number of SCMA iterations	N_{SCMA}
Number of LDPC iterations	N_{LDPC}
Number of information bits	$N_{info.}$
Column weight of the indicator matrix	d_r
Row weight of the indicator matrix	d_c
4 resources \times 4 codewords \times 6 users	$4 \times 4 \times 6$
4 resources \times 16 codewords \times 6 users	$4 \times 16 \times 6$
5 resources \times 4 codewords \times 10 users	$5 \times 4 \times 10$

Throughout the simulation results, standard matrix prototypes of the parity-check matrices [20] for LDPC code are used with the following characteristics: codeword block length $n=648$, subblock size is $Z=27$ and coding rates used are: 1/2, 3/4 and 5/6.

A. Configuration A (4x4x6):

In this configuration, the overload factor is 150% as follows: 4 resources are used to transmit a total of 6 users. Since $M=4$, this means that each user can send / receive $\log_2(M) = \log_2(4) = 2$ bits. With transmitted data of $6 \times 2 = 12$ bits per block. CBs in [24] are used in the above configuration.

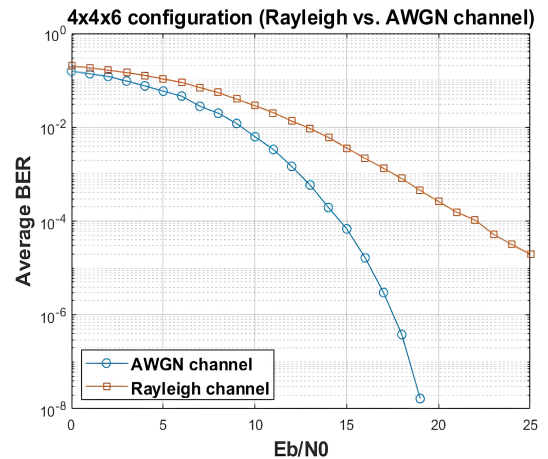


Fig. 7. BER of Rayleigh channel and AWGN channel in 4x4x6 configuration ($N_{SCMA} = 2$; no LDPC code; Number of frames = 1000).

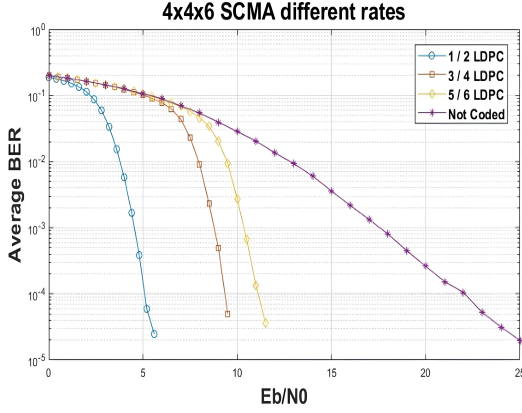


Fig. 8. BER for different LDPC rates in 4x4x6 configuration in Rayleigh channel ($N_{SCMA} = 2$; $N_{LDPC} = 12$; codeword block length = 648 bits; subblock size = 27)

In Fig. 7, the effect of Rayleigh channel on the average (6 users average) BER is demonstrated. In AWGN channel, BER of 10^{-4} is at around $E_b/N_0 = 15$ dB. While, in Rayleigh fading channel, BER of 10^{-4} is at $E_b/N_0 = 22$ dB. And to find the effect of Rayleigh channel on $\frac{E_b}{N_0}$:

$$\frac{E_b}{N_0} = \frac{SNR}{\text{Bit Rate}} \quad (18)$$

where SNR is the Signal-to-Noise Ratio and Bit Rate. The formula to convert $\frac{E_b}{N_0}$ to dB is:

$$\frac{E_b}{N_0} (\text{dB}) = 10 \log_{10} \left(\frac{E_b}{N_0} \right) \quad (19)$$

This formula is arranged to solve for $\frac{E_b}{N_0}$:

$$\frac{\hat{E}_b}{N_0} = 10^{\left(\frac{\frac{E_b}{N_0} (\text{dB})}{10} \right)} \quad (20)$$

where $\frac{\hat{E}_b}{N_0}$ is the difference of $\frac{E_b}{N_0}$ between Rayleigh and AWGN at the same BER. So, after putting the results from Fig. 7, then:

$$\frac{\hat{E}_b}{N_0} = 10^{\left(\frac{22-15}{10} \right)} = 10^{0.7} \approx 5 \quad (21)$$

This means that $\frac{E_b}{N_0}$ in Rayleigh channel is five times that in AWGN channel at BER of 10^{-4}

In Fig. 8 the BER of 10^{-4} with Rayleigh channel is at $\frac{E_b}{N_0} = 23$ dB. After adding 1/2 code rate LDPC, BER with the

Algorithm 2 Max-Log-MPA Algorithm

Step 0: Initialization

Initialize the log-domain codewords probabilities:

$\eta_{j \rightarrow k}^0(x_j) = -\log M \quad \forall j = 1, \dots, J, \quad \forall k \in \xi$ where ξ is the set of subcarriers carrying the information of user j .

Step 1: Iterative Message Exchange

for $t = 1$ to N_{SCMA} do

Step 1a: Passing information from RN to UN

for each subcarrier k do

for each user $j \in \zeta$ do

Calculate a_i for $i = 1, \dots, M$:

$$a_i = -\frac{1}{\sigma^2} \|y_k - \sum_{j \in \zeta} h_{kj} x_{kj}\|^2 + \sum_{i \in \zeta \setminus j} \eta_{i,k}^{t-1}(x_i) \quad \forall k = 1, \dots, K, \quad \forall j \in \zeta$$

where ζ is the set of users transmitting on subcarrier k

Calculate $L_{k \rightarrow j}^t(x_j)$ for the given codeword x_j :

$$L_{k \rightarrow j}^t(x_j) = \max_{x_i | i \in \zeta \setminus j} \left(-\frac{1}{\sigma^2} \|y_k - \sum_j h_{kj} x_{kj}\|^2 + \sum_{i \in \zeta \setminus j} \eta_{i \rightarrow k}^{t-1}(x_i) \right)$$

end for

end for

Step 1b: Passing information from UN to RN

for each user j do

for each subcarrier $k \in \xi$ do

Calculate $\eta_{j \rightarrow}^t(x_j)$ for the given codeword x_j :

$$\eta_{j \rightarrow}^t(x_j) = \log \left(\frac{1}{M} \right) + \sum_{i \in \xi \setminus k} L_{i \rightarrow j}^{t-1}(x_i)$$

end for

Normalization step is ignored due to log-domain simplification.

end for

end for

Step 2: LLR Calculation and Bits Estimation

for each user j do

Calculate the log-domain a posteriori probability for the codeword x_j :

$$\log(P_a(x_j)) = \log \left(\frac{1}{M} \right) + \sum_{k \in \xi} L_{k \rightarrow j}^{N_{SCMA}}(x_j)$$

for each bit b_i in x_j do

Calculate the bit-wise LLR:

$$\text{LLR}(b_i) = \max_{x_j \in X: b_i=0} (\log(P_a(x_j))) - \max_{x_j \in X: b_i=1} (\log(P_a(x_j)))$$

Estimate the bit b_i :

$$b_i = \begin{cases} 1, & \text{if } \text{LLR}(b_i) \geq 0 \\ 0, & \text{otherwise} \end{cases}$$

end for

end for

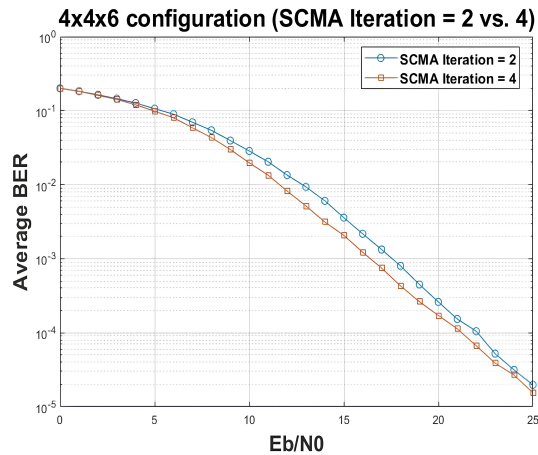


Fig. 9. Comparison between two SCMA iteration numbers in 4x4x6 configuration (Rayleigh channel, without LDPC code).

same value is at $\frac{E_b}{N_0} = 5$ dB. Hence, a gain of 18 dB at the cost of half of the signal being redundant.

In Fig. 9, at $\frac{E_b}{N_0} = 14$, the BER values for 2 and 4 iterations are: 0.00605 and 0.00313, respectively. For only increasing the iterations by factor of two, the BER is decreased by half.

From Fig. 10 it is noted that initially when increasing the iterations number, the BER is significantly reduced, until it reaches SCMA iteration = 5, which gives the lowest BER in the above $\frac{E_b}{N_0}$. After that it reaches a state of saturation, due to a property of any iterative decoding technique; convergency reaches a local minimum. This matches what was shown in [25].

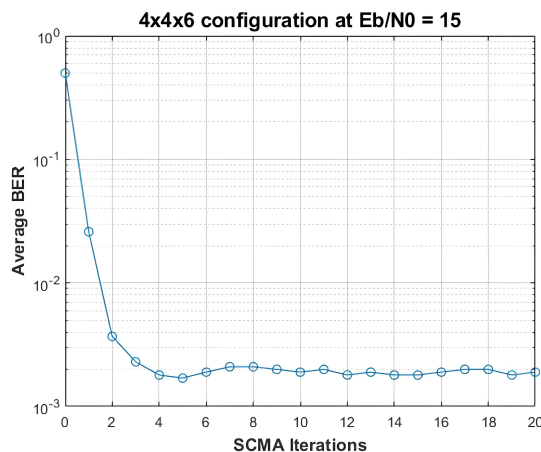


Fig. 10. Different SCMA iteration numbers at a fixed $\frac{E_b}{N_0} = 15$ in 4x4x6 configuration.

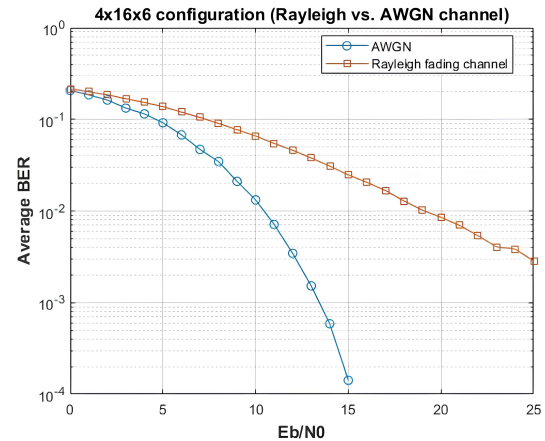


Fig. 11. BER Comparison between Rayleigh channel and AWGN channel in 4x16x6 configuration ($N_{SCMA} = 4$; without LDPC code; Number of frames = 1000).

B. Configuration B (4x16x6):

In this configuration, the number of information bits is doubled. Since, $M=16$ (each CB has 16 unique columns) and $\log_2(16) = 4$ bits. With transmitted data of $6 \times 4 = 24$ bits per block. That increase in information has several effects on the system. Firstly, with more data, more chances of errors. Secondly, with larger data rates, it becomes harder to process the signals. This means, more advanced algorithms are required and more computing power, which make the system more complex and expensive.

In Fig. 11, a BER of 10^{-2} is at E_b/N_0 of 19,10 dB for Rayleigh and AWGN, respectively. that means there is a difference of 9 dB ≈ 5 times AWGN is the Rayleigh effect. And it grows larger when increasing the $\frac{E_b}{N_0}$.

Hence, the use of LDPC code is vital when dealing with large data lengths. Its effect is obvious in Fig. 12. The system reaches a BER of 10^{-3} at $\frac{E_b}{N_0}$ of 5.6,29 dB at 1/2 LDPC code rate and without the use of LDPC code, respectively.

In Fig. 13, one can notice that there is no big difference between 2 and 4 iterations. So, from that, it is concluded that 4 is not the local minimum value. The local minimum value is demonstrated in Fig. 14.

In this figure, the lowest value of BER = 0.02242 is at 16 iterations.

C. Configuration C (5x4x10):

This configuration has 5 resources to transmit 10 users. That means, each resource can be used to carry two users (200% overloading factor), which is double the number of users of normal OMA systems. The information bits for each user are 2 bits per subblock, and the transmitted data is $5 \times 2 = 10$ bits per block.

In Fig. 15, a BER of 10^{-2} is at $\frac{E_b}{N_0}$ of 25,17 dB for Rayleigh

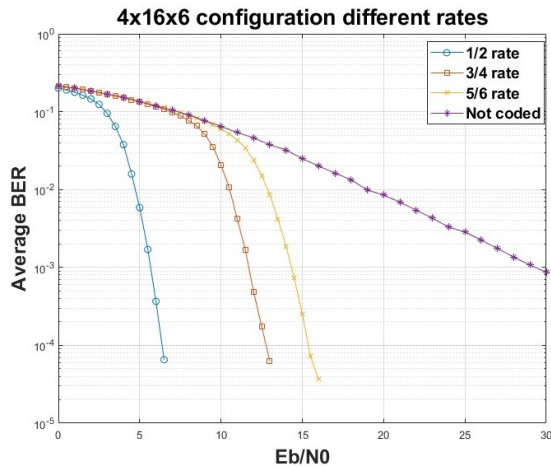


Fig. 12. BER Comparison between different LDPC rates in 4x16x6 in Rayleigh channel ($N_{SCMA}=4$; $N_{LDPC}=12$; codeword block length = 648 bits; subblock size = 27).

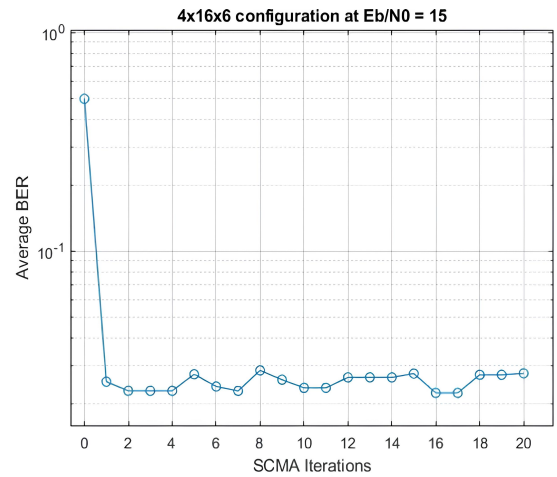


Fig. 14. Different SCMA iteration numbers at a fixed $\frac{Eb}{N0} = 15$ in 4x16x6.

and AWGN, respectively. that means there is a difference of 8 dB ≈ 6.3 .

It is noted from Fig. 16 that the gain of using 17 iterations instead of 2 is about 2 dB ≈ 1.6 .

From Fig. 17, the local minimum BER value = 0.0026 at 17 iterations.

Figure 18 shows a comparison of 10 users over 5 resources for different LDPC code rates.

Comparing the results of Fig. 18 with [26], a clear performance improvement can be noticed for the same Huawei CB. In [26], a BER of 10^{-5} is achieved with perfect channel coefficients at $\frac{Eb}{N0} = 26$. While, in this work, as shown in

Fig. 18, it is achieved at $\frac{Eb}{N0} = 15$ in Rayleigh channel and still gives a gain of 11 dB ≈ 12.5 . Table ?? shows a summary of Rayleigh channel fading results for $\frac{Eb}{N0}$ values in dB at BER = 10^{-3} . The local minimum value of the log-MPA. LDPC gain of a 1/2 code rate in dB. And the total information bits sent per frame (N_{info}), where:

$$N_{info} = V \log_2(M) \times \text{codeword block length} \times \text{code rate} \quad (22)$$

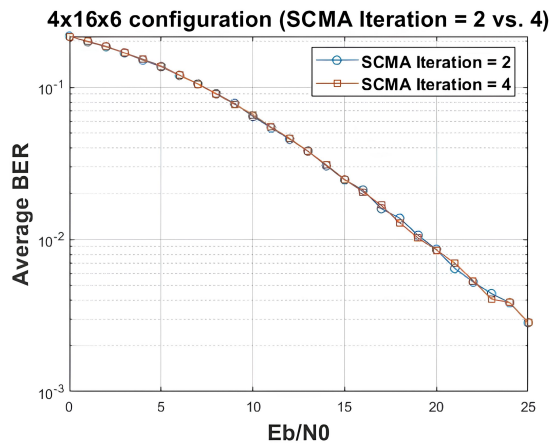


Fig. 13. BER Comparison between two SCMA iteration numbers in 4x16x6 configuration (Rayleigh channel, without LDPC code).

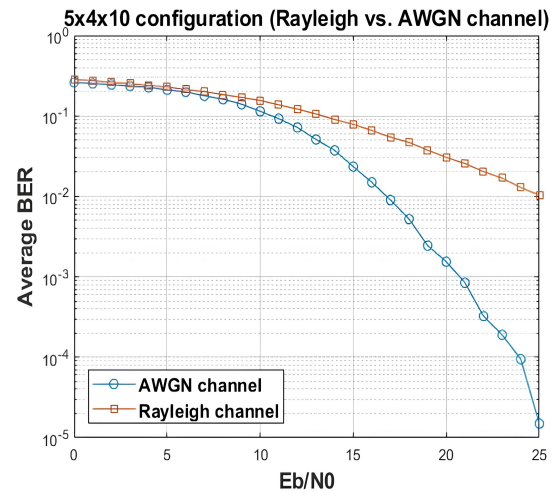


Fig. 15. BER Comparison between Rayleigh channel and AWGN channel in 5x4x10 configuration ($N_{SCMA}=2$; without LDPC code; Number of frames = 10,000).

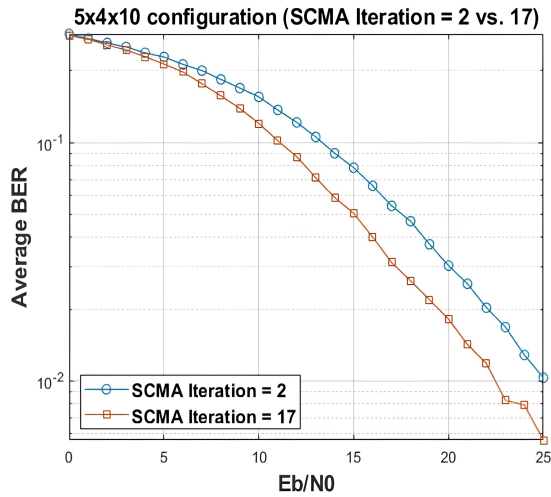


Fig. 16. Comparison between two SCMA iteration numbers in 5x4x10 configuration (Rayleigh channel, without LDPC code).

TABLE III. SUMMARY OF DIFFERENT CONFIGURATIONS' RESULTS CONCERNING E_b/N_0 , LOCAL MINIMUM VALUE, LDPC GAIN AND N_{info} AT $BER = 10^{-3}$.

System (K x M x V)	E_b/N_0 (dB)	Local Minimum Value	LDPC Gain (dB)	N_{info}
4 x 4 x 6	17.5	5	13	3888
4 x 16 x 6	29.1	16	23.5	7776
5 x 4 x 10	35	17	20.5	6480

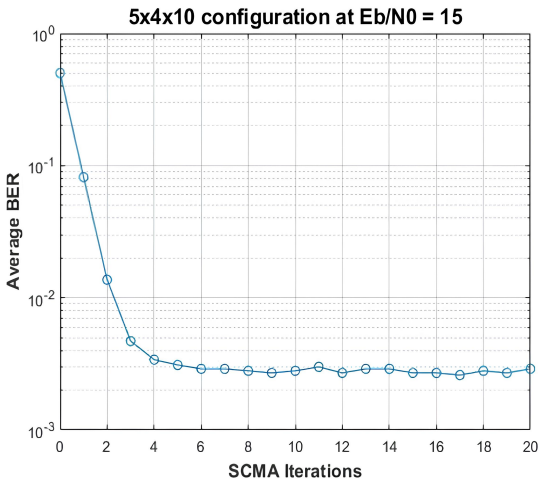


Fig. 17. Different SCMA iteration numbers at a fixed $E_b/N_0 = 15$ in 5x4x10.

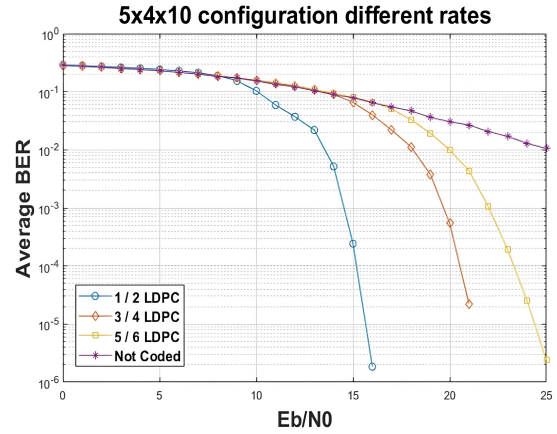


Fig. 18. BER Comparison between different LDPC rates in 5x4x10 in Rayleigh channel ($N_{SCMA} = 2$; $N_{LDPC} = 12$; codeword block length = 648 bits; subblock size = 27).

for Table III, the codeword block length = 648 bits and the code rate is 1/2. Table IV shows a summary of E_b/N_0 values in dB of varying channel conditions at $BER = 10^{-3}$.

TABLE IV. SUMMARY OF E_b/N_0 VALUES IN DB OF VARYING CHANNEL CONDITIONS AT $BER = 10^{-3}$

System (K x M x V)	AWGN Channel	Rayleigh Fading Channel
4 x 4 x 6	12.5	17.5
4 x 16 x 6	13.3	29.1
5 x 4 x 10	20.8	35

Table V shows a summary of E_b/N_0 values in dB of different LDPC rates and without LDPC code so that the performance boost is clear. at $BER = 10^{-3}$ in Rayleigh channel

TABLE V. SUMMARY E_b/N_0 VALUES IN DB OF DIFFERENT LDPC RATES AT $BER = 10^{-3}$ IN RAYLEIGH CHANNEL

System (K x M x V)	1/2	3/4	5/6	Without LDPC code
4 x 4 x 6	4.5	8.8	10.4	17.5
4 x 16 x 6	5.6	11.6	14.4	29.1
5 x 4 x 10	14.5	19.5	22	35

Table VI is a summary of LDPC code Gains in dB for different code rates at $BER = 10^{-3}$ in Rayleigh channel

TABLE VI.
SUMMARY OF LDPC GAINS IN DB FOR DIFFERENT CODE RATES AT $BER = 10^{-3}$ IN RAYLEIGH CHANNEL

System (K x M x V)	1/2	3/4	5/6
4 x 4 x 6	13	8.7	7.1
4 x 16 x 6	23.5	17.5	14.7
5 x 4 x 10	20.5	15.5	13

TABLE VII.
COMPUTATIONAL COST OF SCMA AND LDPC DECODING ITERATION AND COMPARED WITH [27] (IN MILLISECONDS) AT SNR = 12 DB

System (K x M x V)	SCMA	LDPC	Log-MPA without LDPC in [27]
4 x 4 x 6	0.83	7.431	N/A
4 x 16 x 6	1.944	6.28	1.913
5 x 4 x 10	3.95	11.46	N/A

It is worth mentioning that in Table VII, configuration 4x16x6 has less LDPC decoding time when compared to 4x4x6 even though the data rate is doubled. That is because the number of blocks in the former configuration is reduced to half and that leads greater parallelism and faster decoding times.

In Fig. 19 the block length has been increased to 1944, subblock size to 81 and number of iterations to 4. That creates a fair comparison with [28] as shown in Table VIII.

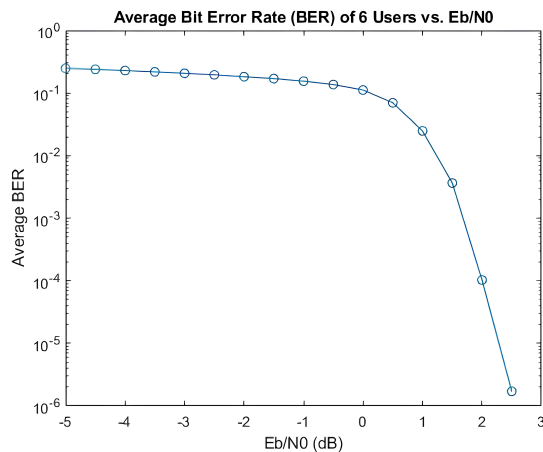


Fig. 19. BER of 4x4x6 in AWGN channel ($N_{SCMA}=4$; $N_{LDPC}=12$; codeword block length = 1944 bits; subblock size = 81).

It is noted that from Table VIII, performance wise, the method used in this paper gives an immense advantage over the methods used in [28] and [13]. the downside is the

complexity when compared to [28]. As in this paper, the number of average float-point real-valued multiplications was 37,744. While in [28] MAP MPA the value was 41,472 which is slightly better, but for Global MMSE-PIC it was 2,640. Which greatly reduces the complexity for real-life implementation at the expense of a lower performance. All values are for $N_{SCMA} = 4$. Thus, this paper aims for a decoding algorithm that offers a trade-off between performance and computational costs. In [28], the complexity achieved by MAP-based MPA for 4x4x6 configuration in terms of floating-points real valued multiplications is around 550,000 operations when $BER = 0.001$ at $SNR = 7$ dB and in this paper, it is 28,033 operations when $BER=0.001$ at $SNR = 4.5$ dB. With the same LDPC code rate and both at $N_{SCMA}=1$. Also, the LDPC effect is obvious and superior to other FECs since the data size is large and greatly reduces the complexity that can be seen in polar or turbo codes as denoted by [13].

VI. CONCLUSION

This paper introduced the performance of three SCMA configurations and gave results in terms of the effect of Rayleigh fading channel, the number of SCMA iterations and LDPC gains for different code rates. Also, it demonstrated the reason behind using LDPC code as an error-correcting code with SCMA. Furthermore, this paper introduced the derivation of equations for LLRs in different configurations. Additionally, this paper showed the performance of log-MPA, which significantly reduced the complexity over conventional Maximum A Posteriori (MAP) decoder. Simulation results showed that the SCMA seems to have a promising future as it can support a higher overall service quality to users with $f_{overload} > 1$, higher spectral efficiencies and lower latency due to the sparsity of the both SCMA and LDPC code.

CONFLICT OF INTEREST

The authors declare that there are no conflicts of interest regarding the publication of this manuscript.

AUTHORS' CONTRIBUTIONS

Mustafa Safwan Moafaq: (Corresponding author) developed the theory, obtained and analyzed the results and wrote the original article draft.

Maher K. Mahmood Al-Azawi: proposed the research problem, supervised it, and participated with editing the article.

REFERENCES

- [1] Y. Zhou, Q. Yu, W. Meng, and C. Li, "SCMA codebook design based on constellation rotation," in *2017 IEEE International Conference on Communications (ICC)*, (Paris, France), pp. 1–6, 2017.
- [2] L. Dai, B. Wang, Y. Yuan, S. Han, C. I, and Z. Wang, "Nonorthogonal multiple access for 5G: Solutions, challenges, opportunities, and future research trends," *IEEE Communication Magazine*, vol. 53, pp. 74–81, Sept. 2015.
- [3] S. M. R. Islam, M. Zeng, and O. A. Dobre, "NOMA in 5G systems: Exciting possibilities for enhancing spectral efficiency," *IEEE 5G Tech Focus*, vol. 1, pp. 1–6, Jun. 2017.
- [4] D. Evans, "The Internet of Things: How the Next Evolution of the Internet is Changing Everything," 2011. [Online].
- [5] R. Hoshyar, R. Razavi, and M. Al-Imari, "LDS-OFDM an Efficient Multiple Access Technique," in *2010 IEEE 71st Vehicular Technology Conference*, (Taipei, Taiwan), pp. 1–5, 2010.
- [6] R. Razavi, R. Hoshyar, M. A. Imran, and Y. Wang, "Information Theoretic Analysis of LDS Scheme," *IEEE Communications Letters*, vol. 15, pp. 798–800, August 2011.
- [7] H. Nikopour and H. Baligh, "Sparse code multiple access," in *2013 IEEE 24th Annual International Symposium on Personal, Indoor, and Mobile Radio Communications (PIMRC)*, (London, UK), pp. 332–336, 2013.
- [8] R. Hoshyar, F. P. Wathan, and R. Tafazolli, "Novel Low-Density Signature for Synchronous CDMA Systems Over AWGN Channel," *IEEE Transactions on Signal Processing*, vol. 56, pp. 1616–1626, April 2008.
- [9] Y. Wu, S. Zhang, and Y. Chen, "Iterative multiuser receiver in sparse code multiple access systems," in *Proc. IEEE ICC*, (London, U.K.), pp. 2918–2923, 2015.
- [10] S. Zhang *et al.*, "Sparse code multiple access: An energy efficient up link approach for 5G wireless systems," in *Proc. IEEE Global Commun. Conf. (GLOBECOM'14)*, (Austin, TX, USA), pp. 4782–4787, 2014.
- [11] Z. Pan, E. Li, L. Zhang, J. Lei, and C. Tang, "Design and Optimization of Joint Iterative Detection and Decoding Receiver for Uplink Polar Coded SCMA System," *IEEE Access*, vol. 6, pp. 52014–52026, 2018.
- [12] B. Tahir, S. Schwarz, and M. Rupp, "BER comparison between Convolutional, Turbo, LDPC, and Polar codes," in *2017 24th International Conference on Telecommunications (ICT)*, (Limassol, Cyprus), pp. 1–7, 2017.
- [13] Y. A. Muhammed and R. Z. Yousif, "Investigating the Effect of Different Channel Coding on the Performance of Sparse Code Multiple Access over AWGN Channel," *Wireless Pers Commun*, 2023.
- [14] C. Berrou, A. Glavieux, and P. Thitimajshima, "Near Shannon limit error-correcting coding and decoding: Turbo-codes," *IEEE Transactions on Communications*, vol. 44, no. 10, pp. 1261–1271, 1993.
- [15] E. Arıkan, "Channel polarization: A method for constructing capacity-achieving codes for symmetric binary-input memoryless channels," *IEEE Transactions on Information Theory*, vol. 55, no. 7, pp. 3051–3073, 2009.
- [16] R. G. Gallager, *Low-Density Parity-Check Codes*. Cambridge, MA: MIT Press, 1963.
- [17] "The Performance Evaluation of Multi User OFDM Orthogonal Chaotic Vector Shift Keying Supported by LDPC," *J. eng. sustain. dev.*, vol. 26, pp. 62–72, May 2022.
- [18] S. Chaturvedi, Z. Liu, V. A. Bohara, A. Srivastava, and P. Xiao, "A Tutorial on Decoding Techniques of Sparse Code Multiple Access," *IEEE Access*, vol. 10, pp. 58503–58524, 2022.
- [19] European Telecommunications Standards Institute, "ETSI Standard EN 302 307 V1.4.1: Digital Video Broadcasting (DVB); Second generation framing structure, channel coding and modulation systems for Broadcasting, Interactive Services, News Gathering and other broadband satellite applications (DVB-S2)," 2005.
- [20] "IEEE Std 802.11-2020 (Revision of IEEE Std 802.11-2016). Part 11: Wireless LAN Medium Access Control (MAC) and Physical Layer (PHY) Specifications. IEEE Standard for Information technology — Telecommunications and information exchange between systems. Local and metropolitan area networks — Specific requirements," 2020.
- [21] D. E. Hocevar, "A reduced complexity decoder architecture via layered decoding of LDPC codes," in *IEEE Workshop on Signal Processing Systems, 2004. SIPS 2004.*, (Austin, TX, USA), pp. 107–112, 2004.
- [22] E. A. Hussien and G. Abdulkareem, "Rayleigh fading channel estimation based on Generalized Regression

TABLE VIII.
COMPARISON OF BER AND $\frac{E_b}{N_0}$ IN (dB) VALUES FOR DIFFERENT LEVELS

BER	$\frac{E_b}{N_0}$ in this paper (LDPC-SCMA Max-log MPA)	$\frac{E_b}{N_0}$ in [28] (MAP MPA)	$\frac{E_b}{N_0}$ in [28] (Global MMSE-PIC)	$\frac{E_b}{N_0}$ in [13] (Joint Polar code (JPC-SCMA))	$\frac{E_b}{N_0}$ in [13] (Joint LDPC code (JLC-SCMA))	$\frac{E_b}{N_0}$ in [13] (Joint turbo code (JTC-SCMA))
10^{-1}	0	5.5	5.8	2.8	4.2	5.9
10^{-2}	1.3	5.9	6.5	3.1	4.7	6.5
10^{-3}	1.8	6.0	6.8	3.6	4.8	6.6

Note: All the above systems have 4 resources, 4 codewords and 6 users. From the 1st → 3rd systems, an LDPC code is used with 1944 blocksize and subblock of 81, $N_{SCMA} = 4$ and code rate = 1/2. The 4th system is coded with a polar code with the following parameters: N = 256, K = 128, $N_{SCMA} = 5$ and code rate = 0.25. The 5th system is the same as 1st → 3rd with the only difference being $N_{SCMA} = 5$. the 5th system has the following specifications: Block length = 4096 bits, random interleaver, Max log-MPA and a code rate of 0.25.

Neural Networks,” *J. eng. sustain. dev.*, vol. 27, Mar. 2023.

- [23] G. A. A.-K. Al-Rubyai, “Diversity Combining for DS CDMA System in a Rayleigh Fading Channel with Three Spreading Codes,” *J. eng. sustain. dev.*, vol. 11, Mar. 2007.
- [24] V. P. Klimentyev and A. B. Sergienko, “Detection of SCMA signal with channel estimation error,” in *2016 18th Conference of Open Innovations Association and Seminar on Information Security and Protection of Information Technology (FRUCT-ISPIT)*, (St. Petersburg, Russia), pp. 106–112, 2016.
- [25] S. ten Brink, “Convergence behavior of iteratively decoded parallel concatenated codes,” *IEEE Transactions on Communications*, vol. 49, pp. 1727–1737, Oct. 2001.
- [26] Z. Liu and L. L. Yang, “Sparse or dense: A comparative study of code-domain NOMA systems,” *IEEE Transactions on Wireless Communications*, vol. 20, pp. 4768–4780, Mar. 2021.
- [27] F. Wei and W. Chen, “Low Complexity Iterative Receiver Design for Sparse Code Multiple Access,” *IEEE Transactions on Communications*, vol. 65, pp. 621–634, Feb. 2017.
- [28] W. C. Sun, Y. C. Su, Y. L. Ueng, and C. H. Yang, “An LDPC-Coded SCMA Receiver With Multi-User Iterative Detection and Decoding,” *IEEE Transactions on Circuits and Systems I: Regular Papers*, vol. 66, pp. 3571–3584, Sept. 2019.